Moving Beyond Boron-based Substituents to Achieve Phosphorescence in Tellurophenes

William Torres Delgado,[†] Christina A. Braun,[†] Michael P. Boone,[†] Olena Shynkaruk,[†] Yanyu Qi,[‡] Robert McDonald,[†] Michael J. Ferguson,[†] Przemyslaw Data,[§,#] Shawan K. C. Almeida,[¶] Inara de Aguiar,[¶] Gabriel L. C. de Souza,[¶] Alex Brown,[†,*] Gang He,[‡,*] and Eric Rivard[†,*]

[†]Department of Chemistry, University of Alberta, 11227 Saskatchewan Drive, Edmonton, Alberta, Canada, T6G 2G2

[§]Department of Physics, Durham University, Durham, UK, DH1 3LE

[#]Faculty of Chemistry, Silesian University of Technology, 44-100 Gliwice, Strzody 9, Poland

[¶]Departamento de Química, Universidade Federal de Mato Grosso, Cuiabá, Mato Grosso, 78060-900, Brazil

[‡]Center for Materials Chemistry, Frontier Institute of Science and Technology, Xi'an Jiaotong University, Xi'an, Shaanxi 710054, People's Republic of China

ABSTRACT: Previous research in our group showed that tellurophenes with pinacolboronate (BPin) units at the 2- and/or 5-positions displayed efficient phosphorescence in the solid state, both in the presence of oxygen and water. In this current study, we show that luminescence from a tellurophene is possible when various aryl-based substituents are present, thus greatly expanding the family of known (and potentially accessible) Te-based phosphors. Moreover, for the green phosphorescent perborylated tellurium heterocycle, 2,3,4,5-TeC_4BPin_4 (**4BTe**), oxygen-mediated quenching of phosphorescence is an important contributor to the lack of emission in solution (when exposed to air); thus this system displays aggregation-enhanced emission (AEE). These discoveries should facilitate the future design of color tunable tellurium-based luminogens.

KEYWORDS: phosphorescence, tellurium, inorganic heterocycles, aggregation enhanced emission, color tuning.

INTRODUCTION

It is becoming clear that the incorporation of heavy inorganic elements within π-conjugated systems can lead to desirable optoelectronic properties.[1-4] For example, polytellurophenes and their molecular heterocyclic surrogates have the potential to yield smaller HOMO-LUMO gaps and improved charge mobility in relation to lighter O, S, or Se containing congeners.[5-14] Another promising domain still largely untapped for exploration is the use of the "heavy atom effect" to promote phosphorescence within main group element-based compounds, including species based on Bi, Sn, Pb and Te;[15-19] a key motivator behind this work is the potential to achieve near 100% device performance in OLEDs.[20-23] Our entry into the field of phosphorescent materials occurred when we noted that tellurophenes with pinacolboronate (BPin) groups attached to the 2- and/or 5-positions of the Te heterocycle exhibited green phosphorescence in the solid state and in the presence of oxygen[24] (conditions that generally quench phosphorescence). Soon after, we were able to tune the color and brightness of emission in the solid state by changing the substituents about a tellurophene ring or via modifying the morphology of the luminescent films.[25-27] A number of structurally novel luminescent (predominantly fluorescent) tellurium complexes have also been synthesized recently.[28-37] Particularly salient examples include the tellurium-containing dibenzobarrelenes prepared by Ishii and coworkers,[33] and fluorescent xanthylium-based tellurones reported by Detty and coworkers.[31]

Thus far, published tellurophene emitters from our laboratories each share a common structural motif: namely, the presence of proximal BPin substituents at the 2- and/or 5-positions of a tellurophene (or benzotellurophene) ring.[24,38] In addition, these compounds have been shown to be non-emissive in aerated solutions, leaving two possible dominant quenching pathways: 1) non-radiative quenching of excited triplet states (T_n) mediated by O_2, and/or 2) non-emissive relaxation modulated through molecular vibration/rotation or solvent interactions. In this paper, we disclose a wide range of new phosphorescent tellurophenes functionalized with aromatic groups of substantially different electronic character. These structural modifications also afforded noticeable changes in emission color. In addition, we show that O_2 quenching of phosphorescence within the perborylated tellurophene 2,3,4,5-TeC_4BPin_4 (**4BTe**) dominates in solution, while in the solid state O_2 quenching is suppressed leading to a 24 % absolute phosphorescence quantum yield. In each case, guiding computational studies from density functional theory (DFT) and time-dependent DFT (TD-DFT) are provided, and they have un-

locked a series of general properties required for emission: involvement of Te based orbitals in light absorption and the presence of energetically close excited singlet and triplet states. Accordingly this study provides an important foundation for the future development of OLEDs based on non-precious main group elements.

RESULTS AND DISCUSSION

A Blue Emissive Tellurophene: Influence of Electron-donating Triphenylamine (TPA) Groups. The green emissive tellurophenes **B-Te-6-B** and **4BTe** containing peripheral pinacolboronate groups were the first room temperature phosphorescent Te heterocycles prepared (Chart 1).[24] Later we noted that replacing one BPin group at the 2-position with a phenyl substituent yielded a considerably stabilized triplet excited state, and afforded red-shifted phosphorescence in the yellow-orange spectral range (**2,4-(PinB)$_2$Ph$_2$C$_4$Te**; λ_{em}= 577 nm).[25]

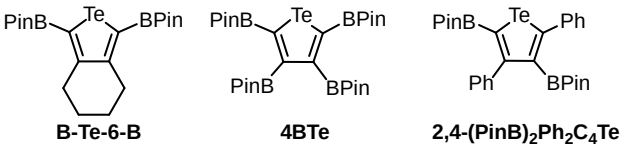

B-Te-6-B **4BTe** **2,4-(PinB)$_2$Ph$_2$C$_4$Te**

Chart 1. Selected phosphorescent tellurophenes prepared by the Rivard group; BPin = pinacolboronate.

Given the widespread use of the triphenylamine (TPA) substituent as an electron donor and two-photon absorbing unit in optoelectronics,[39-41] we decided to investigate the influence on photophysical properties by replacing the BPin substituents in **B-Te-6-B** with TPA groups. Added motivation stemmed from the possible use of these species as hole transporting/electron-blocking layers in perovskite solar cells.[42-44] The synthesis of the triphenylamine (TPA) derivative **TPA-Te-6-TPA** proceeded via a similar zirconium-mediated alkyne coupling protocol (Scheme 1) as previously reported.[24-28,45-48] This reaction yields the five-membered ZrC$_4$ zirconacycle **TPA-ZrCp$_2$-6-TPA** as an intermediate species which can be directly converted *in situ* into the target tellurophene via Zr/Te transmetallation (Scheme 1) with the Te(II) source[49] Bipy•TeCl$_2$ (Bipy = 2,2′-bipyridine).

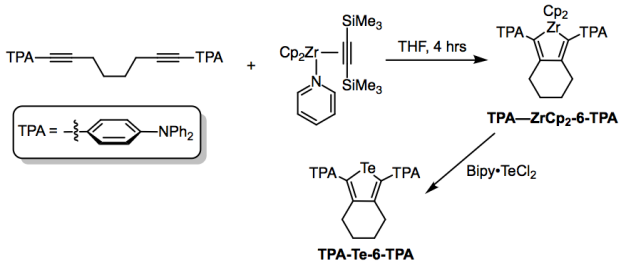

Scheme 1. Synthesis of the triphenylamine (TPA)-capped tellurophene TPA-Te-6-TPA.

The electron-rich tellurophene **TPA-Te-6-TPA** exhibits an intense UV-Vis absorption band in THF centered at 306 nm (ε = 2.86 × 10^4 M^{-1} cm^{-1}) that is flanked by a broad absorption at *ca.* 350 nm extending to 450 nm (Figure S7).[50] When a THF solution of **TPA-Te-6-TPA** is irradiated at 362 nm in air, deep blue luminescence transpires in the form of a broad emission profile at 485 nm (absolute quantum yield (Φ) = 11.9 %; Figure 1). The accompanying emission lifetime[50] (τ) of 2.3 ns is in the range expected for fluorescence. We also noted some aggregation-caused quenching (ACQ) when a sample of **TPA-Te-6-TPA** was suspended in water/THF mixtures (Figure S11);[50] this behavior is in contrast to what is found in structurally related BPin-substituted tellurophenes (*e.g.* **B-Te-6-B**) which show pronounced aggregation-induced emission (AIE) in air.[24,51] Interestingly, green emission occurs when **TPA-Te-6-TPA** is irradiated at 365 nm in the solid state under ambient conditions (Figure S12, λ_{em} = 525 nm).[50] As anticipated from the ACQ found in aggregates, the intensity of the solid state emission of **TPA-Te-6-TPA** was very low, thus obviating the recording of reliable quantum yield and lifetime data. Importantly, we were able to demonstrate energy transfer between the triplet sensitizer benzophenone and **TPA-Te-6-TPA** in the solid state, thus adding support for the assignment of weak phosphorescence in **TPA-Te-6-TPA** (see Figures S26 and S27).[50] The closest congener to **TPA-Te-6-TPA** reported in the literature is 2,5-bis(TPA)thiophene which emits blue light (λ_{em} = 438 nm) when irradiated at 386 nm in THF.[52] While still very rare, examples of blue-emitting tellurium species are starting to appear in the literature. For example, Ishii and coworkers noted that very weak blue fluorescence in THF was possible (Φ < 0.01) at room temperature from a Te-containing dibenzobarrelene.[33] In addition, a water soluble 2,5-diarylatedtellurium(VI) oxide (RC$_6$H$_4$)Te(O)$_2$C$_4$H$_2$(C$_6$H$_4$R) (R = -O-(CH$_2$CH$_2$O)$_8$Me) was shown to be blue luminescent by the Seferos group.[32]

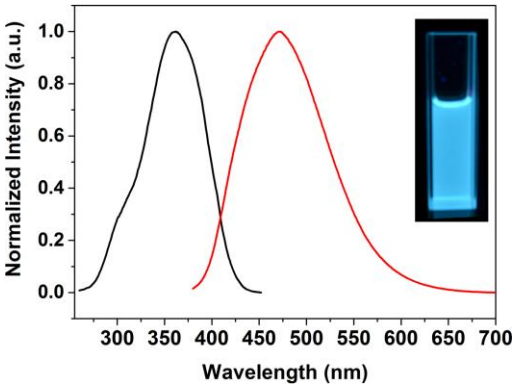

Figure 1. Excitation (black line) and emission (red line) spectra of **TPA-Te-6-TPA** in THF (1.0 × 10^{-5} M); λ_{ex} = 362 nm.

Solid State Phosphorescence from Non-borylated Tellurophenes: A Next Generation Class of Phosphor. Intrigued by the possible phosphorescence of **TPA-Te-6-TPA** in the solid state, we decided to prepare electronically distinct tellurophenes and benzotellurophenes. Accordingly, a TPA substituent was incorporated as part of a donor-acceptor (D-A) motif within a benzotellurophene scaffold.[25] Heating the readily available zirconocene Cp$_2$ZrPh$_2$ in the presence of the new

alkyne reagent Ph_2N-C_6H_4-C≡C-BPin (TPA-C≡C-BPin), led to the expected extrusion of benzene and the regioselective formation of the desired benzozirconocene **Benzo-ZrCp$_2$(BPin)TPA** (Scheme 2); this species was then converted *in situ* into the D-A benzotellurophene **Benzo-Te(BPin)TPA** by the subsequent addition of Bipy•$TeCl_2$. The resulting off-white solid was obtained in an overall isolated yield of 80 % and showed a coplanar arrangement between the BPin ring and the benzotellurophene core (Figure 2); the remaining aryl substituent that joins the TPA group to the Te heterocycle is twisted by 51.9(4)°. A similar structural motif was noted within the solid state phosphorescent emitter **Benzo-Te(BPin)Ph**.[25] Another salient structural feature is the long intermolecular Te--Te distances in **Benzo-Te(BPin)TPA** and the shortest contact confirmed by X-ray crystallography is 4.36 Å. This value lies just outside the sum of the van der Waals radii for Te (4.12 Å),[53] and thus one might expect phosphorescence in the solid state due to a suppression of triplet-triplet annihilation (self-quenching).

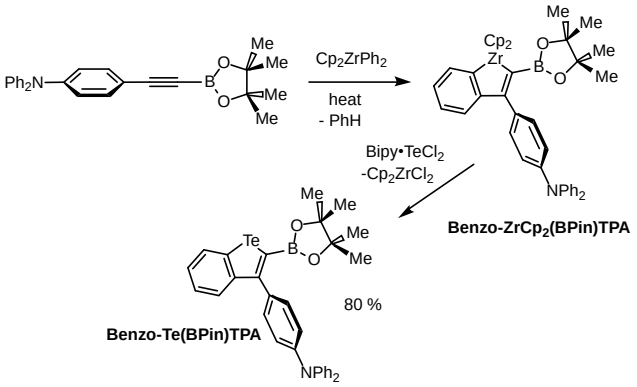

Scheme 2. Preparation of the donor-acceptor (D-A) benzotellurophene, Benzo-Te(BPin)TPA.

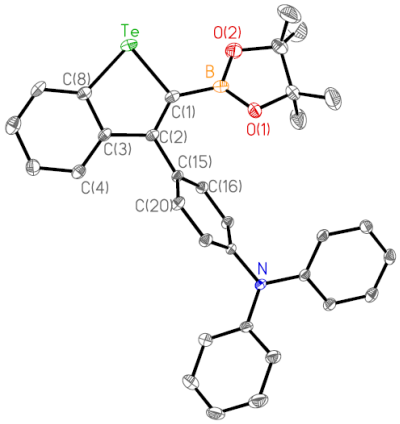

Figure 2. Molecular structure of **Benzo-Te(BPin)TPA** with thermal ellipsoids presented at a 30 % probability level. All hydrogen atoms have been omitted for clarity. Selected bond lengths (Å) and angles (°): Te-C(1) 2.079(3), Te-C(8) 2.058(4), C(1)-C(2) 1.361(4), C(2)-C(3) 1.464(4), C(8)-C(3) 1.411(4); C(8)-Te-C(1) 82.07(13), Te-C(1)-B 117.7(2), Te-C(1)-C(2) 112.4(2), C(1)-C(2)-C(3) 117.5(3), C(2)-C(3)-C(8) 116.2(3), C(3)-C(8)-Te 111.8(2).

The optoelectronic properties of **Benzo-Te(BPin)TPA** were measured and some notable differences were found in relation to the known phenylatedbenzotellurophene **Benzo-Te(BPin)Ph**.[25] The UV-Vis spectrum of **Benzo-Te(BPin)TPA** in THF exhibits a strong absorption at 294 nm in addition to an overlapping weaker absorption at 361 nm (Figure S13).[50] This benzotellurophene was non-emissive when excited at 365 nm (both in THF and CH_2Cl_2). However bright yellow-orange emission occurs when this compound is irradiated at 390 nm in the solid state in air (λ_{em} = 595 nm; Φ = 7.0 %; τ = 15.7 μs) (Figure 3), in line with what has been found in our previously reported phosphorescent tellurophenes.[24-28] Phosphorescence in **Benzo-Te(BPin)TPA** was also confirmed by triplet sensitization experiments with benzophenone (Figures S21 and S22),[50] while no change in emission profile was noted when the luminescence of **Benzo-Te(BPin)TPA** in a PMMA matrix was measured (Figure S24)[50] thus ruling out excimer-based emission. For comparison, substantially blue-shifted phosphorescence (λ_{em} = 520 nm; green emission) is seen in the weakly emitting phenylated-congener **Benzo-Te(BPin)Ph**.[25] Thus it appears that incorporating a donor-acceptor motif into a benzotellurophene scaffold promotes the anticipated bathochromic shift of emission. We are currently exploring extended π-structures (*e.g.* anthracene and phenanthrene) bearing the same emissive motif as in **Benzo-Te(BPin)TPA** to red-shift the emission even further and to eventually improve charge transport for possible OLED-based applications.

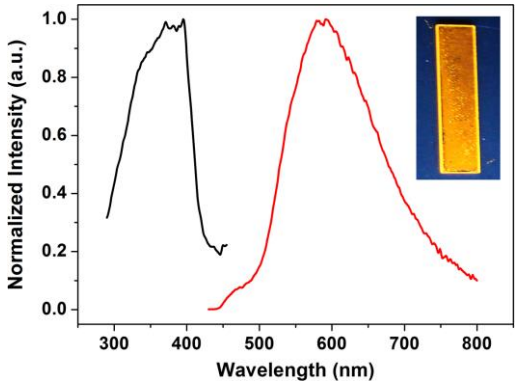

Figure 3. Excitation (black line) and emission (red line) spectra of **Benzo-Te(BPin)TPA** in the solid state; drop-cast films from THF; λ_{ex} = 390 nm.

We also prepared the electron-rich tellurophene **TeC$_4$(2-thienyl)$_4$** (Scheme 3) as a pale yellow solid via a two-step alkyne coupling/transmetallation protocol starting from 1,2-bis(2-thienyl)acetylene.[54] The structure of **TeC$_4$(2-thienyl)$_4$** is shown in Figure 4 and yields a set of flanking coplanar thiophene units with respect to the central TeC_4 heterocycle, while the remaining thiophene rings are twisted. Somewhat to our surprise, this species is non-emissive both in solution (THF) and in the solid state. This is in contrast to the tetrakis(thienyl)-substituted germole (biphenyl)GeC_4(2-thienyl)$_4$ that exhibits bright yellow emission in the solid state.[55] The closest intermolecular Te--Te distance in **TeC$_4$(2-thienyl)$_4$** is 4.09 Å, which is *ca.* 0.2 Å shorter than in **Benzo-Te(BPin)TPA**. While these slightly shorter contacts could be instigating enhanced triplet-triplet annihilation, another explanation could be a difference in film crystallinity[27] between the

two compounds. Prior work in our group showed that amorphous films of **B-Te-6-B** were much less emissive than crystalline ones, presumably due to an increase in O_2 diffusion and phosphorescence quenching in air.[27] As will be discussed in detail later, each of the reported Te heterocycles have energetically close excited singlet (S_n) and triplet (T_n) states, according to TD-DFT computations; thus, intersystem crossing (ISC) and phosphorescence should be possible. However as will be seen, the involvement of Te based orbitals during light absorption is also needed to promote ISC.

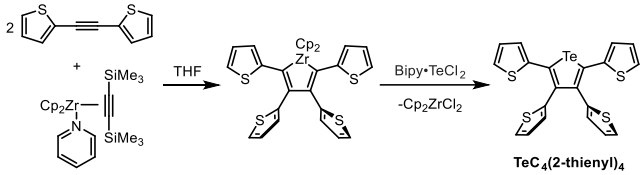

Scheme 3. Synthesis of the non-emissive thienyl-substituted tellurophene, TeC_4(2-thienyl)$_4$.

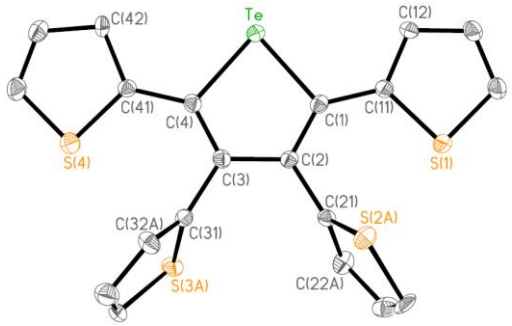

Figure 4. Molecular structure of **TeC_4(2-thienyl)$_4$** with thermal ellipsoids presented at a 30 % probability level. All hydrogen atoms have been omitted for clarity. Selected bond lengths (Å) and angles (°): Te-C(1) 2.071(5), Te-C(4) 2.087(5), C(2)-C(3) 1.443(8), C(2)-C(21) 1.493(7), C(4)-C(41) 1.447(8); C(1)-Te-C(4) 81.9(2), Te-C(1)-C(11) 117.3(4), Te-C(4)-C(41) 117.3(4).

Given the versatility of the synthetic route used to obtain our Te heterocycles, we decided to take advantage of this method to install electronically distinct naphthyl, fluorenyl and fluoroaryl aromatic groups at the 2,5-positions about a tellurophene. Starting from the known BPin-capped tellurophene **B-Te-6-B**,[6] effective Suzuki-Miyaura coupling was possible with various arylbromide reagents (Scheme 4) to give 2,5-diarylated tellurophenes. Use of MeCN or MeCN/THF solvent, K_2CO_3 base, and a $Pd(OAc)_2$/XPhos pre-catalyst mixture was needed to suppress protodeboronation within **B-Te-6-B**.[28] The target tellurophenes **Naph-Te-6-Naph**, **Fl-Te-6-Fl** and **Ar^F-Te-6-Ar^F** (Naph = 2-naphthyl; Fl = 2-fluorenyl; Ar^F = 3,5-$(F_3C)_2C_6H_3$) were obtained as air- and moisture-stable light brown to yellow solids in moderate isolated yields (36 to 58 %).

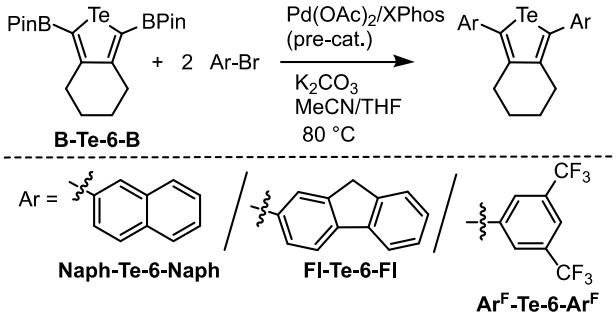

Scheme 4. Modular syntheses of 2,5-diarylated tellurophenes via Suzuki-Miyaura cross-coupling.

High-quality crystals of both the naphthyl and fluoroaryl (Ar^F) analogues **Naph-Te-6-Naph** and **Ar^F-Te-6-Ar^F** were obtained, and the resulting refined structures by X-ray crystallography are presented in Figures 5 and 6. The core tellurophene arrays in each species have metrical parameters consistent with other known tellurophene heterocycles,[6,24,25] while the 2-naphthyl groups in **Naph-Te-6-Naph** adopt canted arrangements with respect to the central TeC_4 heterocycle (by 39.2(6)° and 60.1(8)°). As with the thiophene-capped analogue **TeC_4(2-thienyl)$_4$**, the closest solid state Te--Te interaction in **Naph-Te-6-Naph** (4.01 Å) lies at the edge of the sum of van der Waals radii for Te;[53] likewise the emission of the naphthyl analogue is minimal at room temperature (Figure S29).[50] Cooling a film of **Naph-Te-6-Naph** to 77 K under nitrogen led to very weak phosphorescence, as described below.

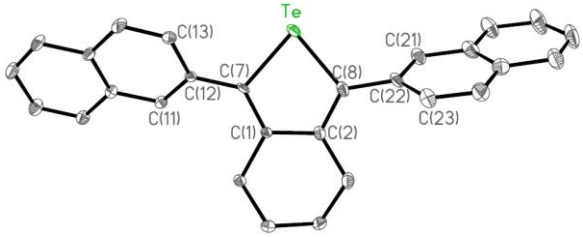

Figure 5. Molecular structure of **Naph-Te-6-Naph** with thermal ellipsoids presented at a 30 % probability level. All hydrogen atoms have been omitted for clarity. Selected bond lengths (Å) and angles (°): C(7)-Te 2.088(7), C(8)-Te 2.079(8), C(1)-C(2) 1.463(10), C(2)-C(8) 1.349(10), C(1)-C(7) 1.359(10); C(7)-Te-C(8) 81.5(3), Te-C(7)-C(12) 118.9(5), Te-C(8)-C(22) 120.7(6); torsion angles (°):Te-C(7)-C(12)-C(11) 140.8(6), Te-C(8)-C(22)-C(23) 119.9(8).

Each of the aryl-linked tellurophenes **Naph-Te-6-Naph**, **Fl-Te-6-Fl** and **Ar^F-Te-6-Ar^F** show primary absorptions (λ_{max}) in the narrow range of 312-350 nm (Figure S9)[50] in THF, and are non-emissive in solution. These species, however, exhibit luminescence consistent with aggregation-induced phosphorescence.[56,57] In the case of the naphthyl and fluorenyl counterparts **Naph-Te-6-Naph** and **Fl-Te-6-Fl**, cooling of the films to 77 K was needed to observe orange emission at 588/634 nm and 633 nm, respectively (Figures 7 and 8), tentatively assigned as phosphorescence on the basis of the large Stokes

shift. Unfortunately the emission intensities were still too low to allow an adequate estimate of reliable lifetimes. In the case of **Naph-Te-6-Naph**, addition of benzophenone (to give a 1:1 mixture) as a triplet sensitizer enable detection of the same emission profile at room temperature as seen at 77K, providing added evidence for phosphorescence in **Naph-Te-6-Naph** (Figure S28)[50,58] The bis(trifluoromethyl)benzene-capped tellurophene **Ar^F-Te-6-Ar^F** was much more brightly emissive and gave yellow phosphorescence at 595 nm (λ_{ex} = 375 nm; Φ = 9.5%; τ = 29.3μs) in the solid state (Figures 9 and S28).[50] When one examines the solid state structure of **Ar^F-Te-6-Ar^F** (Figure 6), a similar overall geometry is present as in the naphthyl congener **Naph-Te-6-Naph**, with twisting of the proximal 3,5-$(F_3C)_2C_6H_3$ rings by *ca.* 60° with respect to the planar tellurophene ring. However the added steric bulk imposed by the $-CF_3$ groups leads to substantial elongation of the shortest intermolecular Te--Te distance to 4.62 Å, which should assist in preventing self-quenching in the triplet excited state via triplet-triplet annihilation (TTA). Consistent with a lack of excimer formation, the emission properties of **Ar^F-Te-6-Ar^F** in a PMMA matrix yielded similar emission data as the pure tellurophene (Figure S19).[50] In prior work, it was also shown that when aryl substituents were positioned adjacent to a tellurophene ring, stabilization of the excited triplet state (T_1) occurs in relation to their borylated (BPin) analogues, leading to a red-shift in emission;[25] thus it appears that a similar effect is occurring within **Ar^F-Te-6-Ar^F** and this further demonstrates the ability to control the color of emission for this class of phosphors.

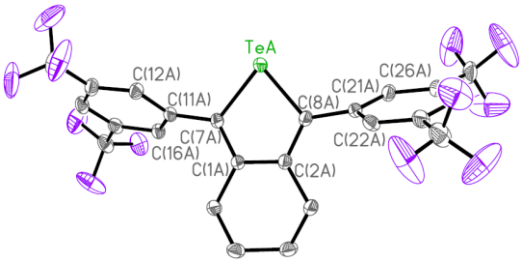

Figure 6. Molecular structure of **Ar^F-Te-6-Ar^F** with thermal ellipsoids presented at a 30 % probability level. All hydrogen atoms have been omitted for clarity. Selected bond lengths (Å) and angles (°); values due to a second molecule in the asymmetric unit are listed in square brackets: Te-C(7) 2.068(3) [2.069(3)], Te-C(8) 2.068(3) [2.075(3)], C(1)-C(2) 1.449(4) [1.452(4)], C(1)-C(7) 1.366(4) [1.360(4)], C(2)-C(8) 1.366(4) [1.361(4)]; C(7)-Te-C(8) 81.66(12) [81.48(12)], Te-C(7)-C(11) 122.3(2) [121.9(2)], Te-C(8)-C(21) 124.8(3) [121.3(2)]; torsion angles: C(1)-C(7)-C(11)-C(12) 115.8(4) [119.6(4)], Te-C(8)-C(21)-C(22) 114.5(3) [127.1(3)].

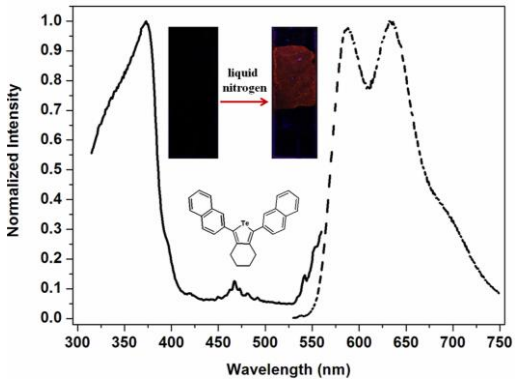

Figure 7. Excitation (black line) and emission (dashed line) spectra of **Naph-Te-6-Naph** at 77K in the solid state; drop-cast film from THF; λ_{ex} = 375 nm.

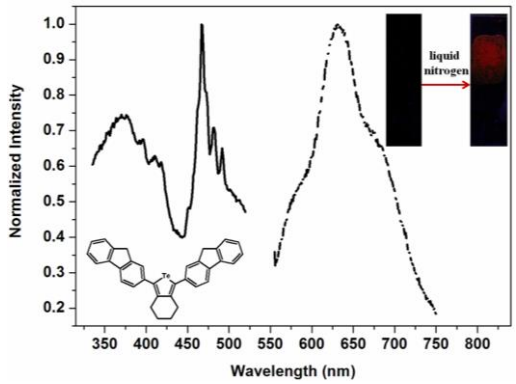

Figure 8. Excitation (black line) and emission spectra (dashed line) of **Fl-Te-6-Fl** at 77K in the solid state; drop-cast film from THF; λ_{ex} = 475 nm.

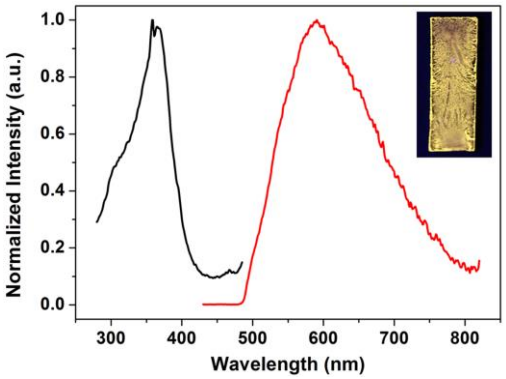

Figure 9. Excitation (black line) and emission (red line) spectra of **Ar^F-Te-6- Ar^F** at room temperature, in air; drop-cast film from THF; λ_{ex} = 375 nm.

An interesting effect was noted when the luminescence of the known tellurophene **4BTe** (Chart 1) was explored in rigorously degassed solutions. As shown in Figure S14,[50] noticeable phosphorescence (λ_{em} = *ca.* 570 nm) can be found in deaerated solutions of **4BTe** in THF, toluene and methylcyclohexane with relative phosphorescence quantum yields of 2, 2, and 6%, respectively [phosphorescence lifetimes (τ_{Ph}) = 0.6 μs, 9.6 μs, and 10.8 μs, respectively]. In each case, very weak

fluorescence was also noted with lifetimes in the 1.3 to 20.7 ns time regime[50] and emission maxima centered at 420 nm. For comparison, the absolute phosphorescence quantum yield of **4BTe** in the solid state is much greater with a value of 20% in air vs. 24% under argon (Figure S15).[50] These are the highest phosphorescence quantum yields observed thus far for an emissive tellurophene, and suggest that in the film state both diffusion related quenching by O_2 and intermolecular (TTA) self-quenching of triplet states in **4BTe** is substantially reduced, as would be expected from the long Te--Te separation of 9.44 Å found in the solid state structure of **4BTe**.[24] Accordingly the emission profile of **4BTe** as a 1 wt% mixture in Zeonex (Figure S18)[50] remained unaltered compared with that of pure **4BTe**, again ruling out excimer-based emission. The solid state phosphorescence lifetimes of **4BTe** under both air and argon atmosphere were each modeled with biexponential decays (Figures S16 and S17)[50] and yielded lifetime values of 89.5 and 210 μs (45:55 ratio) in air, and 196 and 455 μs (26:74 ratio) under argon. Thus it appears that in **4BTe**, the turn-on of ambient (air) phosphorescence in the solid state stems from limiting the diffusion of O_2 to excited triplet states, rather than solely restriction of intramolecular rotation/vibration (as is often found in aggregation-induced emission).[51]

Computational Investigations: Added Insight into the Nature of Luminescence in Aryl-functionalized Te-Heterocycles. A likely mechanism for phosphorescence in the reported Te heterocycles is initial photoexcitation to an excited singlet (S_1) state, followed by intersystem crossing to an energetically similar triplet (T_n) state, with final phosphorescence from the lowest T_1 state.[59] The excited states of **4BTe**, its lighter sulfur and selenium congeners **4BS** and **4BSe**,[50] and the newly reported compounds in this paper have been examined using a combination of DFT (B3LYP/cc-pVTZ-(PP))[50] for ground state structure optimization and TD-DFT (B3LYP/cc-pVTZ-(PP))[50] for excited state computations; for selected compounds spin-unrestricted DFT (UB3LYP/cc-pVTZ-(PP))[50] was used for structure optimization of the lowest energy triplet state. Previous work[26] demonstrated that these were suitable choices of functional and basis set for studying Te heterocycles.

In the case of the initially prepared Te phosphor **B-Te-6-B**, a combination of the "heavy atom effect" (*i.e.*, increased spin-orbit coupling from Te) and energetically close S_1 and T_3 states, enables effective intersystem crossing, and eventual phosphorescence from the T_1 state to transpire.[26] Not too surprisingly, a similar energetic profile is seen in **4BTe** (Figure 10) wherein computations in the gas phase, and simulated THF and $CHCl_3$ solvent environments (with polarizable continuum models) all show excitation to an S_1 state that is within 0.14 eV of a T_3 state; assuming Kasha's rule is followed,[60] rapid decay to the T_1 state then transpires, followed by phosphorescence. The related sulfur and selenium analogues $EC_4(BPin)_4$ (E = S and Se; **4BS** and **4BSe**)[50] also showed similar S_1 to T_3 energy level trends, with only 0.02 and 0.18 eV energy differences between each set of states, respectively (Figure 10).[50] However irradiation of these lighter chalcogenophenes[28] in the absence of O_2 did not lead to any detectable phosphorescence both in solution or in the solid state. Thus it is possible that the expected enhanced spin-orbit coupling in the Te congener **4BTe** allows intersystem crossing and phosphorescence to occur.

The structurally distinct benzotellurophene **Benzo-TeBPin(TPA)** was also studied computationally; however, using B3LYP, the major absorption predicted was at too long a wavelength. Subsequently, some charge transfer character upon excitation was noted based on examination of the associated orbitals (Figure S34)[50] and a charge transfer diagnostic (Table S6). Hence, additional TD-DFT computations were carried out with the CAM-B3LYP and M06-2X functionals. These results demonstrated that the long wavelength peak observed experimentally at 350 nm (3.54 eV) corresponded to a weak excitation to S_1 and also a much stronger excitation to S_2 (see Tables S7 and S8); the excitation to S_2 involves a mixture (primarily) of HOMO to LUMO and HOMO-1 to LUMO excitation (see Table S9 and the corresponding orbitals in Figures S35 and S36).[50] The computed absorption spectra of **Benzo-TeBPin(TPA)** using either CAM-B3LYP or M06-2X match well with the experimentally obtained UV-Vis spectrum in THF (Figure S7).[50] Quite interesting were the results obtained from the computed singlet and triplet vertical excitation energies of **Benzo-TeBPin(TPA)** (results here refer to those from CAM-B3LYP in THF). The energy of the S_1/S_2 states (3.76 eV and 3.86 eV) are energetically quite close to a series of excited triplet states (T_6-T_8; 3.60 to 3.89 eV), with the closest states being T_7/T_8 (3.74 eV and 3.89 eV); thus based on energetics alone, there are multiple possible pathways by which intersystem crossing (ISC) to the triplet manifold can occur, in line with the noted phosphorescence of **Benzo-TeBPin(TPA)** seen in the solid state.

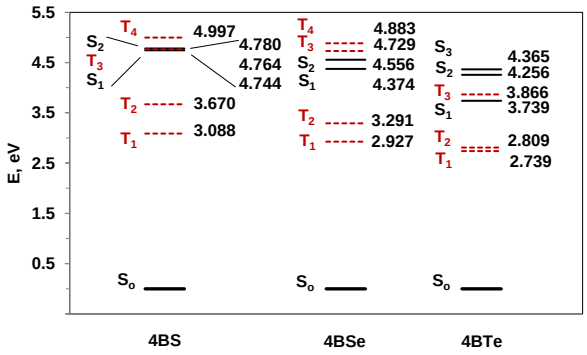

Figure 10. Computed vertical excitation energies to both singlet and triplet states at the TD-B3LYP/cc-pVTZ (cc-pVTZ-PP for Te) level of theory in the gas phase for **4BS**, **4BSe** and **4BTe**.

When one computes vertical excitation energies for the remaining tellurophenes discussed in this article, **TeC_4(2-thienyl)$_4$**, **TPA-Te-6-TPA**, **Naph-Te-6-Naph**, **Fl-Te-6-Fl** and **Ar^F-Te-6-Ar^F**, the S_1 states (and sometimes allowed transitions to S_2 and S_3 states) are each within *ca.* 0.1 eV of various T_n states (see Tables S4, S11, S13, S14, and S16 for the computed energy values).[50] As a result the energy requirements for ISC appear to have been met for all compounds studied, especially when one considers the possibility for enhanced spin-orbit coupling in the presence of Te. However, taking into account the nature of the excitation to S_1 for the non-phosphorescent (**TeC_4(2-thienyl)$_4$** and **TPA-Te-6-TPA**) versus phosphorescent compounds, a clear trend emerges: in those compounds that are phosphorescent, a strong low-energy absorption (*i.e.*, one with the highest oscillator strength) al-

ways involves excitation from an orbital strongly localized on the Te center (see corresponding orbital plots in the SI, Figures S35, S36, and S37).[50] On the other hand, for the non-phosphorescent compounds, the low-energy absorption does not originate from the Te center (see corresponding orbital plots in the SI, Figures S22 and S26);[50] the difference in the nature of the excitation is most readily observed when comparing the non-phosphorescent **TeC_4(2-thienyl)$_4$** and **TPA-Te-6-TPA** with the analogous phosphorescent **4BTe** and **B-Te-6-B** compounds (see Figure S32 in the present SI and Figure S32 of Ref. 24, respectively). Thus it appears that attaining intense phosphorescence depends on both the suppression of O_2 quenching in the solid state and the presence of substantial orbital participation from Te during photoexcitation.[61]

CONCLUSIONS

By taking advantage of a general zirconium-mediated synthesis of tellurium heterocycles, a new series of phosphorescent benzotellurophenes and tellurophenes containing aryl-substituents were prepared. Importantly this work shows that boryl substituents (such as BPin)[24,38] are not essential to achieve solid state phosphorescence in air, thus greatly expanding the number of potential phosphors that can be accessed in the future. In addition, computational studies helped highlight a general trend where the most intensely phosphorescent compounds show photoexcitation from a localized Te orbital. Moreover, these species each possess multiple energetically similar triplet excited states in relation to the excited singlet state(s) occupied upon photoexcitation, thus enhancing the chance for the requisite intersystem crossing prior to phosphorescence. Lastly, the observed emission of these Te heterocycles in the solid state appears to be facilitated by the suppression of triplet quenching by O_2 rather than solely the restriction of intramolecular rotation/vibration and prevention of triplet-triplet annihilation. Future work will involve incorporation of these emitting cores into π-extended (and polymeric) structures along with the incorporation of related heavy main group elements[1] into emissive arrays.

EXPERIMENTAL SECTION

General Methods. Unless explicitly stated, all reactions were conducted with standard Schlenk and glove box (MBraun) techniques using N_2 as an inert atmosphere, with solvents that were dried using a Grubbs' type purification system[61,62] manufactured by Innovative Technology Inc. 1,7-Octadiyne was purchased from GFS Chemicals, Cp_2ZrCl_2 was purchased from Strem Chemicals Inc., 2-isopropoxy-4,4,5,5-tetramethyl-1,3,2-dioxa-borolane (^{i}PrOBPin), 1-bromo-3,5-bis(trifluoromethyl)benzene and trimethylsilylacetylene were purchased from Matrix Scientific, and all other chemicals were obtained from Aldrich. Commercially obtained chemicals were used as received except for pyridine, which was freshly distilled under nitrogen from potassium hydroxide. Cp_2ZrPh_2,[63] Ph_2N-C_6H_4-C≡CH,[64] bis(cyclopentadienyl)zirconium-2,3,4,5-tetra(2-thienyl)methanide (Cp_2ZrC_4(2-thienyl)$_4$),[55] Cp_2Zr(pyridine)($Me_3SiCCSiMe_3$),[65] 2-ethynylthiophene,[66] 4-bromophenyl-*N*-*N*′-diphenylamine,[67] Bipy•$TeCl_2$,[49] **B-Te-6-B**[6] and **EC_4(BPin)$_4$** (E = S, Se and Te)[6,28] were synthesized according to literature procedures. ^{1}H,^{13}C{^{1}H},^{11}B{^{1}H} and ^{19}F NMR spectra were recorded on either a Varian Inova 500 or 400 spectrometer and referenced externally to Me_4Si (^{1}H and ^{13}C{^{1}H}), F_3B•OEt_2 (^{11}B) and $CFCl_3$ (^{19}F). Melting points were measured with a MelTemp apparatus and are reported without correction. Elemental analyses were performed by the Analytical and Instrumentation Laboratory at the University of Alberta. UV-Visible spectroscopic measurements were performed with a Varian Cary 300 Scan spectrophotometer and fluorescence measurements with a Photon Technology International (PTI) MP1 fluorometer and for photoluminescence lifetimes on a time-correlated single photon counting fluorescence spectrometer (Edinburgh Instruments FLS920) using an EPL-375 picosecond pulsed diode laser with vertical polarization (70.3 ps pulse width) as an excitation source; absolute quantum yields were measured with an integrating sphere system within the same fluorescence spectrometer. Thermogravimetric analysis was performed under nitrogen atmosphere on a Perkin Elmer Pyris 1 TGA. High-resolution mass spectra were obtained on an Agilent 6220 spectrometer and Kratos Analytical MS-50G system. Solution phosphorescence, prompt fluorescence, and delayed fluorescence spectra and decays were recorded using nanosecond gated luminescence and lifetime measurements (from 400 ps to 1 s) using either a high energy pulsed Nd:YAG laser emitting at 355 nm (EKSPLA) or a N_2 laser emitting at 337 nm. Emission was focused onto a spectrograph and detected on a sensitive gated iCCD camera (Stanford Computer Optics) having sub-nanosecond resolution. Solution photoluminescence spectra of **4BTe** were obtained on a Horiba Jobin Yvon Fluorolog 3 spectrofluorometer; absorption spectra on a Shimadzu UV-3600 UV-Vis-NIR spectrophotometer. Fluorescence excitation spectra were recorded in relation to the emission maximum, and fluorescence emission spectra were recorded at the excitation maximum. The quantum yields of **4BTe** in solution were estimated by comparison with a quantum yield standard (9,10-diphenylantracence and tetraphenylporphyrin).[68,69]

Synthesis of TPA-C≡C-$(CH_2)_4$-C≡C-TPA (1). 1,7-Octadiyne (0.319 g, 3.00 mmol) was added to 4-bromophenyl-*N*,*N*-diphenylamine (2.000 g, 6.169 mmol), $(Ph_3P)_2PdCl_2$ (0.239 g, 0.340 mmol), CuI (0.130 g, 0.680 mmol), PPh_3 (0.178 g, 0.680 mmol), and ^{i}Pr$_2$NH (35 mL) in a Teflon-capped 100 mL Schlenk bomb. The reaction flask was sealed, partially evacuated, and heated at 100 °C for 12 hrs, after which the reaction mixture was cooled to room temperature and the volatiles were removed *in vacuo*. The resulting residue was taken up in 100 mL of Et_2O, filtered through a pad of Celite and the solvent was removed from the filtrate *in vacuo* to afford a yellow oil. This residue was triturated with 1 mL of pentane to yield **TPA-C≡C-$(CH_2)_4$-C≡C-TPA (TPA-C_8-TPA)** as a pale yellow powder (1.522 g, 86 %). ^{1}H NMR (500 MHz, $CDCl_3$): δ 7.27-7.20 (m, 12H, Ar*H*), 7.10-6.99 (m, 12H, Ar*H*), 6.97-6.91 (m, 4H, Ar*H*), 2.45 (br, 4H, -CC-C*H*$_2$-CH$_2$CH$_2$-C*H*$_2$-CC-), 1.46 (br, 4H, -CC-CH$_2$-C*H*$_2$C*H*$_2$-CH$_2$-CC-). ^{13}C{^{1}H} NMR (126 MHz, $CDCl_3$): δ 147.5 (Ar*C*), 132.6 (Ar*C*), 129.4 (Ar*C*), 124.8 (Ar*C*), 124.3 (Ar*C*), 123.3 (Ar*C*), 123.0 (Ar*C*), 117.4 (Ar*C*), 89.1 (alkyne), 81.0 (alkyne), 28.1 (-*C*H$_2$CC-), 19.2 (-*C*H$_2$*C*H$_2$-). HR-MS (ESI) ($C_{44}H_{36}N_2$): m/z; Calcd: 592.2878. Found: 592.2871 (Δ ppm = 1.2).

Synthesis of TPA-Te-6-TPA (2). To a solution of Cp_2Zr(pyridine)($Me_3SiCCSiMe_3$) (0.368 g, 0.780 mmol) in 5 mL of THF was added a solution of **TPA-C_8-TPA** (**1**) (0.472 g, 0.797 mmol) in 5 mL of THF. This reaction mixture was allowed to stir for 4 hrs, after which a solution of Bipy•$TeCl_2$ (0.302 g, 0.877 mmol) in 3 mL of THF was added. After 12 hrs, the reaction mixture was filtered through a small plug of silica gel, and the filtrate concentrated to dryness to give a pale green residue. This product was dissolved in 1 mL of a 2:1 CH_2Cl_2/hexanes mixture, filtered through a plug of silica gel to yield a yellow solution. Removal of the solvent from the filtrate afforded **TPA-Te-6-TPA** as a spectroscopically pure yellow solid (0.354 g, 63 %). ^{1}H NMR (500 MHz, C_6D_6): δ 7.30-7.24 (m, 4H, Ar*H*), 7.14-7.10 (m, 8H, Ar*H*), 7.08-7.02 (m, 12H, Ar*H*), 6.89-6.83 (m, 4H, Ar*H*), 2.64 (br, 4H, -C-C*H*$_2$-CH$_2$CH$_2$-C*H*$_2$-C), 1.38 (br, 4H, -C-CH$_2$-C*H*$_2$C*H*$_2$-CH$_2$-C-). ^{13}C{^{1}H} NMR (126 MHz, C_6D_6): δ 148.3 (Ar*C*), 147.0 (Ar*C*), 144.2 (Ar*C*), 139.3 (Ar*C*), 135.2 (Ar*C*), 130.6 (Ar*C*), 129.7 (Ar*C*), 125.0 (Ar*C*), 123.8 (Ar*C*), 123.3 (Ar*C*), 30.9 (-C-*C*H$_2$-CH$_2$CH$_2$-*C*H$_2$-C), 23.6 (-C-CH$_2$-*C*H$_2$*C*H$_2$-CH$_2$-C). HR-MS (MALDI) ($C_{44}H_{36}N_2Te$): m/z; Calcd: 722.1940. Found: 722.1935 (Δppm = 0.7). TGA: T_{dec} = 299 °C. UV-Vis (in THF): $\lambda_{max}(\varepsilon)$ = 306 nm (2.86×10^4 $M^{-1}cm^{-1}$), shoulder at λ = 350 nm. Fluorescence emission (THF) (λ_{ex} = 362nm): λ_{em} = 485 nm, absolute fluorescence quan-

tum yield: Φ = 11.9 %; lifetime (1.0×10^{-5} M solution in THF): τ = 2.3 ns. Emission (film) (λ_{ex} = 365nm): λ_{em} = 525 nm; Intensity is too low to give reliable lifetime and absolute quantum yield. Anal. Calcd. for $C_{44}H_{36}N_2Te$: C, 73.36; H, 5.04; N, 3.89; Found: C, 72.75; H, 5.05; N, 3.84. Mp (°C): decomposes above 140 °C.

Synthesis of TPA-C≡C-BPin (3). ^{n}BuLi (2.5 M solution in hexanes, 0.80 mL, 2.0 mmol) was added to a cold (-78 °C) solution of Ph_2N-C_6H_4-C≡CH (0.516 g, 1.92 mmol) in 30 mL of Et_2O at -78 °C and the mixture was stirred at this temperature for 0.5 hrs before warming to room temperature over 1 hr. After this timeframe, the reaction mixture was cooled back down to -78 °C and ^{i}PrOBPin (0.392 g, 2.11 mmol) was added in one portion, and the reaction mixture was allowed to warm to room temperature while stirring overnight (12 hrs). The mixture was then cooled back down to -78 °C and HCl (2.0 M solution in Et_2O, 1.2 mL, 2.4 mmol) was added followed by stirring for 2 hrs at room temperature. The reaction mixture was filtered and the volatiles were removed from the filtrate to leave an oily residue. The resulting oil was triturated with 1 mL of pentane to afford **TPA-C≡C-BPin** as an off-white solid (0.215 g, 28 %). ^{1}H NMR (500 MHz, $CDCl_3$): δ 7.36 (d, 2H, $^3J_{HH}$ = 9.0 Hz, Ar*H*), 7.30-7.27 (m, 4H, Ar*H*), 7.12-7.05 (m, 6H, Ar*H*), 6.92 (d, 2H, $^3J_{HH}$ = 9.0 Hz, Ar*H*), 1.32 (s, 12H, -C*H*$_3$). ^{13}C{^{1}H} NMR (176 MHz, $CDCl_3$): δ 149.1 (Ar*C*), 147.0 (Ar*C*), 133.8 (Ar*C*), 129.6 (Ar*C*), 125.6 (Ar*C*), 125.2 (Ar*C*), 124.1 (Ar*C*), 121.3 (Ar*C*), 114.1 (alkyne), 84.4 (-*C*CH$_3$), 24.9 (-*C*H$_3$). ^{11}B{^{1}H} NMR (160 MHz, $CDCl_3$): δ 30.1 (br). HR-MS (EI) ($C_{26}H_{26}BNO_2$): m/z; Calcd: 395.2057. Found: 395.2057 (Δppm = 0.0).

Synthesis of Benzo-Te(BPin)TPA (4). **TPA-C≡C-BPin** (**3**) (0.187 g, 0.473 mmol), Cp_2ZrPh_2 (0.166 g, 0.500 mmol), and 5 mL of THF were loaded into a Teflon-capped Schlenk bomb, partially evacuated, sealed, and heated to 100 °C for 16 hrs. Afterwards, the reaction mixture was brought into the glove box and transferred into a scintillation vial. To this mixture was added solid Bipy•$TeCl_2$ (0.195 g, 0.550 mmol) and the reaction mixture allowed to stir for 12 hrs. The volatiles were then removed under vacuum, and the remaining solid dissolved in 1 mL of CH_2Cl_2/hexanes (2:1) and filtered through a short plug of silica gel. The solvent was removed from the filtrate *in vacuo* to yield **Benzo-Te(BPin)TPA** as a pure off-white solid (0.228 g, 80 %). Crystals of **Benzo-Te(BPin)TPA** suitable for X-ray analysis were obtained by slow evaporation of a CH_2Cl_2/hexanes solution. ^{1}H NMR (500 MHz, $CDCl_3$): δ 8.02 (d, 1H, $^3J_{HH}$ = 7.7 Hz, benzo-*H*), 7.64 (d, 1H, $^3J_{HH}$ = 7.7 Hz, benzo-*H*), 7.35 (t, 1H, $^3J_{HH}$ = 8.0 Hz, benzo-*H*), 7.29-7.24 (m, 7H, Ar*H* and benzo-*H*), 7.18 (d, 4H, $^3J_{HH}$ = 7.5 Hz, Ar*H*), 7.15 (d, 2H, $^3J_{HH}$ = 8.0 Hz, Ar*H*), 7.03 (t, 2H, $^3J_{HH}$ = 7.5 Hz, Ar*H*), 1.23 (s, 12H, -C*H*$_3$). ^{13}C{^{1}H} NMR (126 MHz, $CDCl_3$): δ 157.4 (Ar*C*), 149.4 (Ar*C*), 148.1 (Ar*C*), 147.1 (Ar*C*), 135.9 (Ar*C*), 135.2 (Ar*C*), 132.4 (Ar*C*), 131.1 (Ar*C*), 129.7 (Ar*C*), 129.3 (Ar*C*), 125.4 (Ar*C*), 124.9 (Ar*C*), 124.1 (Ar*C*), 124.0 (Ar*C*), 122.7 (Ar*C*), 84.1 (-*C*CH$_3$), 24.8 (-*C*H$_3$).^{11}B{^{1}H} NMR (160 MHz, $CDCl_3$): δ 30.6 (br). UV-Vis (in THF): $\lambda_{max}(\varepsilon)$ = 294 nm (2.42×10^4 M^{-1}cm^{-1}), 361 nm (1.11×10^4 M^{-1}cm^{-1}). Emission (film) (λ_{ex} = 390 nm): λ_{em} = 595 nm, absolute emission quantum yield: Φ = 7.0 %; τ = 15.7 μs. Anal. Calcd. for $C_{32}H_{30}BNO_2Te$: C, 64.16; H, 5.05; N, 2.34; Found: C, 63.80; H, 5.31; N, 2.33. TGA: T_{dec} = 257 °C. Mp (°C): > 230.

Modified synthesis of (2-thienyl)C≡C(2-thienyl) (5). To a solution of 2-bromothiophene (0.43 mL, 4.4 mmol) in dry Et_3N (20 mL) were added $PdCl_2(PPh_3)_2$ (0.056 g, 0.080 mmol), PPh_3 (0.042 g, 0.16 mmol), CuI (0.031 g, 0.16 mmol), and 2-ethynylthiophene (0.433 g, 4.00 mmol). After stirring for 16 hrs at 70 °C, the volatiles were removed *in vacuo* and the residue was dissolved in CH_2Cl_2 (50 mL) and filtered through a 1 cm plug of silica gel. The solvent was removed from the filtrate and the crude product was purified by column chromatography (loaded as a 5 mL solution in CH_2Cl_2, silica gel, hexanes as an eluent, R_f = 0.73) to yield **(2-thienyl)C≡C(2-thienyl)** as a white solid (0.433 g, 57 %). The corresponding ^{1}H and ^{13}C{^{1}H} NMR spectral data matched those reported previously in the literature.[70]

Synthesis of TeC_4(2-thienyl)$_4$ (6). Cp_2ZrC_4(2-thienyl)$_4$(0.151 g, 0.25 mmol) and Bipy•$TeCl_2$ (0.098 g, 0.28 mmol) were dissolved in 6 mL of THF and the resulting mixture was allowed to stir at room temperature for 24 hrs. A dark green solution formed over a black precipitate; this precipitate was allowed to settle and the mother liquor was filtered through a 1 cm plug of silica gel. The volatiles were removed from the filtrate and the resulting crude product was purified by column chromatography (silica gel, THF:pentane = 1:2 as the eluent, R_f = 0.70) to yield **TeC_4(2-thienyl)$_4$** as the green powder which was further washed with hexanes (2 × 5 mL) at room temperature to give **TeC_4(2-thienyl)$_4$** as a light yellow solid (0.037 g, 33 %). X-ray quality crystals of **TeC_4(2-thienyl)$_4$** were obtained from slow evaporation of a THF/pentane solution at room temperature. ^{1}H NMR (400 MHz, $CDCl_3$): δ 7.28 (dd, $^3J_{HH}$ = 5.1 Hz, $^4J_{HH}$ = 1.1 Hz, 2H, Thienyl*H*), 7.14 (dd, $^3J_{HH}$ = 5.1 Hz, $^4J_{HH}$ = 1.2 Hz, 2H, Thienyl*H*), 6.90-6.92 (two overlapping dd, $^3J_{HH}$ = 3.5 Hz, $^4J_{HH}$ = 1.2 Hz, 4H, Thienyl*H*), 6.86 (dd, $^3J_{HH}$ = 5.1 Hz, $^4J_{HH}$ = 3.7 Hz, 2H, Thienyl*H*), 6.82 (dd, $^3J_{HH}$ = 3.5 Hz, $^4J_{HH}$ = 1.2 Hz, 2H, Thienyl*H*).^{13}C{^{1}H} NMR (100 MHz, $CDCl_3$): δ 142.0, 140.7, 140.3, 134.9, 129.5, 127.7, 127.0, 126.9, 126.6 (Thienyl-*C*). UV-Vis (in THF): $\lambda_{max}(\varepsilon)$ = 394 nm (1.81×10^4 M^{-1}cm^{-1}). UV-Vis (film): λ_{max}= 386 and 427 (shoulder) nm. HR-MS (EI) ($C_{20}H_{12}S_4Te$): m/z; Calcd.: 509.8884. Found: 509.8871 (Δppm = 2.5). Anal. Calcd. for $C_{20}H_{12}S_4Te$: C, 47.27; H, 2.38; S, 25.24; Found: C, 47.12; H, 2.51; S, 25.30. TGA: T_{dec} = 296 °C. Mp(°C): 196-197.

Synthesis of Naph-Te-6-Naph (7). **B-Te-6-B** (0.201 g, 0.41 mmol), 2-bromonaphthalene (0.175 g, 0.82 mmol), $Pd(OAc)_2$ (3.7 mg, 4 mol %), XPhos (0.016 g, 8 mol %) were dissolved in 5.0 mL of MeCN. After adding 0.82 mL of aqueous K_2CO_3 (2.0 M solution, 1.6 mmol), the reaction mixture was stirred at 80 °C for 60 hrs. The final product was not soluble in MeCN, thus the supernatant was decanted and 50 mL of $CHCl_3$ was added to dissolve the precipitate. The resulting solution was filtered through a pad of Celite. After the volatiles were removed from the filtrate, the remaining solid was washed three times with 20 mL aliquots of pentane to remove the residual XPhos and the remaining product was dried under reduced pressure to afford **Naph-Te-6-Naph** as a pure brown solid (0.072 g, 36 %). X-ray quality crystals were obtained by slow evaporation of a solution of the compound in a toluene/hexanes mixture at room temperature. ^{1}H NMR (600 MHz, $CDCl_3$): δ 7.89 (s, 2H, Ar*H*), 7.88-7.82 (m, 6H, Ar*H*), 7.61-7.57 (m, 2H, Ar*H*), 7.53-7.47 (m, 4H, Ar*H*), 2.82 (br, 4H, C=CC*H*$_2$), 1.69 (br, 4H, C=CCH$_2$C*H*$_2$). ^{13}C{^{1}H} NMR (500 MHz, $CDCl_3$): δ 144.9, 139.7, 137.9, 133.5, 132.3, 128.1, 128.01, 127.96, 127.9, 127.8, 126.5 and 126.1 (Ar*C* and Te-*C*=*C*), 30.8 (C=CCH$_2$*C*H$_2$) and 23.5 (C=C*C*H$_2$CH$_2$). UV-Vis (in THF): $\lambda_{max}(\varepsilon)$ = 281 nm (2.21×10^4 M^{-1}cm^{-1}), 324 nm (1.85×10^4 M^{-1}cm^{-1}). HR-MS (EI) ($C_{28}H_{22}Te$): m/z; Calcd.: 488.0784. Found: 488.0778 (Δppm = 1.1). Anal. Calcd. for $C_{28}H_{22}Te$: C, 69.19; H, 4.56; Found: C, 68.47; H, 4.59. Mp(°C): 171-174.

Synthesis of Fl-Te-6-Fl (8). **B-Te-6-B** (0.174 g, 0.36 mmol), 2-bromofluorene (0.183 g, 0.71 mmol), $Pd(OAc)_2$ (3.2 mg, 4 mol %), XPhos (0.014 g, 8 mol %) were dissolved in 4.4 mL of MeCN. After adding 0.9 mL of aqueous K_2CO_3 (2.0 M solution, 1.7 mmol), the reaction mixture was stirred at 80 °C for 3.5 days. The resulting mixture was poured into 50 mL of $CHCl_3$ while stirring and then filtered through a pad of Celite. The filtrate washed three times with 100 mL portions of H_2O. The organic layer was dried over $MgSO_4$, filtered and the volatiles were removed under reduced pressure. The remaining solid was washed three times with 50 mL portions of cold (~ 0 °C) hexanes to yield **Fl-Te-6-Fl** as a light yellow powder (0.117 g, 58 %). ^{1}H NMR (500 MHz, $CDCl_3$): δ 7.78 (pseudo t, 4H, J_{HH} = *ca.* 8.1 Hz, Ar*H*), 7.61 (pseudo d, 2H, J_{HH} = *ca*. 0.9 Hz, Ar*H*), 7.55 (d, 2H, J_{HH} = *ca.* 7.2 Hz, Ar*H*), 7.47 (dd, 2H, J_{HH} = *ca.* 7.8 Hz, J_{HH} = *ca.* 1.7 Hz, Ar*H*), 7.39 (pseudo t, 2H, J_{HH} = *ca.* 7.3 Hz, Ar*H*), 7.31 (pseudo t, 2H, J_{HH} = *ca.* 7.3 Hz, J_{HH} = *ca.* 1.2 Hz, Ar*H*), 3.94 (s, 4H, C*H*$_2$ in Fl), 2.79 (m, 4H, C=CC*H*$_2$CH$_2$), 1.68 (m, 4H, C=CCH$_2$C*H*$_2$). ^{13}C{^{1}H} NMR (500 MHz, $CDCl_3$): δ 144.6, 143.6,143.5, 141.5, 140.6, 139.8,

139.0, 128.3, 127.0, 126.9, 126.1, 125.2, 120.0 and 119.7 (Ar*C*), 37.1 (*C*H_2), 30.8 (C=C*C*H_2CH$_2$), 23.5 (C=CCH$_2$*C*H_2). UV-Vis (in THF): $\lambda_{max}(\varepsilon)$ = 266 nm (3.07×10^4 M^{-1}cm^{-1}), 330 nm (3.26×10^4M^{-1}cm^{-1}). HR-MS (EI) ($C_{34}H_{26}Te$): m/z; Calcd.: 564.1091. Found: 564.1088 (Δppm = 0.5). Anal. Calcd. for $C_{34}H_{26}Te$: C, 72.64; H, 4.66; Found: C, 71.99; H, 4.82. Mp(°C): > 250.

Synthesis of Ar^F-Te-6-Ar^F (9). **B-Te-6-B** (0.196 g, 0.40 mmol), 5-bromo-1,3-bis(trifluoromethyl)benzene (0.239 g, 0.80 mmol), $Pd(OAc)_2$ (3.6 mg, 4 mol %), XPhos (0.016 g, 8 mol %) were dissolved in 5.5 mL of a solvent mixture of MeCN / THF (10:1) in a vial suitable for microwave reactions. After adding 0.2 mL of aqueous K_2CO_3 (2.0 M solution, 0.4 mmol), the reaction mixture was stirred at 110 °C for 3 hrs in a microwave reactor. The resulting mixture was poured into 60 mL of $CHCl_3$ while stirring, filtered through a pad of Celite and the solvent removed under reduced pressure. The remaining solid was dissolved in 50 mL of toluene and washed four times with 50 mL portions of water. The organic layer was dried over $MgSO_4$, filtered and the volatiles removed under reduced pressure to yield the product as a light yellow solid (0.190 g, 72 %). The resulting crude product was purified by column chromatography using silica gel and petroleum ether as an eluent to give **Ar^F-Te-6-Ar^F** as a pure light yellow solid (0.114 g, 43 %). X-ray quality crystals were obtained by slow evaporation at room temperature of a solution of the compound in hexanes.^{1}H NMR (500 MHz, $CDCl_3$): δ 7.82 (s, 6H, Ar*H*), 2.65 (m, 4H, C=CCH_2CH$_2$), 1.68 (m, 4H, C=CCH$_2$CH_2). ^{13}C{^{1}H} NMR (500 MHz, $CDCl_3$): δ 143.3, 142.2, 137.0 (Ar*C*), 132.0 (quartet, $^2J_{CF}$ = 33.5 Hz, *C*CF$_3$), 129.2 (ArC), 123.3 (quartet, $^1J_{CF}$ = 272.7 Hz, *C*F$_3$), 30.4 (C=C*C*H$_2$CH$_2$), 23.0 (C=CCH$_2$*C*H$_2$). ^{19}F NMR (500 MHz, $CDCl_3$): δ 62.8. UV-Vis (in THF): $\lambda_{max}(\varepsilon)$ = 312 nm (1.40×10^4 M^{-1}cm^{-1}). Emission (film) (λ_{ex} = 375 nm): λ_{em} = 600 nm, absolute emission quantum yield: Φ = 9.5 %; τ = 29.3 μs. HR-MS (EI) ($C_{24}H_{14}F_{12}Te$): m/z; Calcd.: 659.9961. Found: 659.9955 (Δppm = 0.8). Anal. Calcd. for $C_{24}H_{14}F_{12}Te$: C, 43.81; H, 2.14; Found: C, 43.99; H, 2.29. Mp(°C): 135-136.

ASSOCIATED CONTENT

Supporting Information

^{1}H, ^{13}C{^{1}H}, ^{19}F{^{1}H} NMR spectra for all of the compounds and crystallographic data for **Benzo-Te(TPA)BPin**, **TeC$_4$(2-thienyl)$_4$**, **Naph-Te-6-Naph**, **Ar^F-Te-6-Ar^F**, and **SeC$_4$(BPin)$_4$**; additional computational details and luminescence data. The Supporting Information is available free of charge on the ACS Publications website at DOI: 10.1021/acsami.xxxxxxx

^{1}H, ^{13}C{^{1}H}, ^{19}F{^{1}H} NMR spectra for all of the compounds (PDF).
Computational details and luminescence data (PDF)
Crystallographic data (CIF)

AUTHOR INFORMATION

Corresponding Authors

*E-mail: erivard@ualberta.ca, alex.brown@ualberta.ca, ganghe@mail.xjtu.edu.cn

Notes

The authors declare no competing financial interest.

ACKNOWLEDGMENTS

This work was supported by the Natural Sciences and Engineering Research Council (NSERC) of Canada (Discovery and CREATE grants to E.R.; Discovery grant to A.B.; postgraduate scholarship to C.A.B.), the Conselho Nacional de Desenvolvimento Científico e Tecnológico (CNPq) of Brazil (Special visiting researcher grant 400179/2014-8 to G.L.C.S. and A.B.), and the Canada Foundation for Innovation. M.P.B. acknowledges the Killam Trust for a Postdoctoral Fellowship. We thank Compute Canada for access to computational resources. We are also grateful to Prof. Yu Fang (Key Laboratory of Applied Surface and Colloid Chemistry, Shaanxi Normal University) for his assistance with the luminescence measurements. P.D. also thanks the European Union's Horizon 2020 research and innovation program under grant agreement No. 691684. E.R. also thanks the Alexander von Humboldt Foundation for an Experienced Researcher Fellowship.

REFERENCES

(1) Parke, S. M.; Boone, M. P.; Rivard, E. Marriage of Heavy Main Group Elements with π-Conjugated Materials for Optoelectronic Applications. *Chem. Commun.* **2016**, *52*, 9485-9505.

(2) Chivers, T.; Laitinen, R. S. Tellurium: A Maverick Among the Chalcogens. *Chem. Soc. Rev.* **2015**, *44*, 1725-1739.

(3) Carrera, E. I.; Seferos, D. S. Semiconducting Polymers Containing Tellurium: Perspectives Toward Obtaining High-Performance Materials. *Macromolecules* **2015**, *48*, 297-308.

(4) Baumgartner, T.; Réau, R. Organophosphorus π-Conjugated Materials. *Chem. Rev.* **2006**, *106*, 4681-4727.

(5) Jahnke, A. A.; Howe, G. W.; Seferos, D. S. Polytellurophenes with Properties Controlled by Tellurium-Coordination. *Angew. Chem., Int. Ed.* **2010**, *49*, 10140-10144.

(6) He, G.; Kang, L.; Torres Delgado, W.; Shynkaruk, O.; Ferguson, M. J.; McDonald, R.; Rivard, E. The Marriage of Metallacycle Transfer Chemistry with Suzuki−Miyaura Cross-Coupling to Give Main Group Element-Containing Conjugated Polymers. *J. Am. Chem. Soc.* **2013**, *135*, 5360-5363.

(7) Jahnke, A. A.; Djukic, B.; McCormick, T. M.; Buchaca Domingo, E.; Hellmann, C.; Lee, Y.; Seferos, D. S. Poly(3-alkyltellurophene)s Are Solution-Processable Polyheterocycles. *J. Am. Chem. Soc.* **2013**, *135*, 951-954.

(8) Park, Y. S.; Kale, T. S.; Nam, C.-Y.; Choi, D.; Grubbs, R. B. Effects of Heteroatom Substitution in Conjugated Heterocyclic Compounds on Photovoltaic Performance: From Sulfur to Tellurium. *Chem. Commun.* **2014**, *50*, 7964-7967.

(9) Jung, E. H.; Bae, S.; Yoo, T. W.; Jo, W. H. The Effect of Different Chalcogenophenes in Isoindigo-Based Conjugated Copolymers on Photovoltaic Properties. *Polym. Chem.* **2014**, *5*, 6545-6550.

(10) Ashraf, R. S.; Meager, I.; Nikolka, M.; Kirkus, M.; Planells, M.; Schroeder, B. C.; Holliday, S.; Hurhangee, M.; Nielsen, C. B.; Sirringhaus, H.; McCulloch, I. Chalcogenophene Comonomer Comparison in Small Band Gap Diketopyrrolopyrrole-Based Conjugated Polymers for High-Performing Field-Effect Transistors and Organic Solar Cells. *J. Am. Chem. Soc.* **2015**, *137*, 1314-1321.

(11) Al-Hashimi, M.; Han, Y.; Smith, J.; Bazzi, H. S.; Alqaradawi, S. Y. A.; Watkins, S. E.; Anthopoulos, T. D.; Heeney, M. Influence of the Heteroatom on the Optoelectronic Properties and Transistor Performance of Soluble Thiophene-, Selenophene- and Tellurophene–Vinylene Copolymers. *Chem. Sci.* **2016**, *7*, 1093-1099.

(12) Razzell-Hollis, J.; Fleischli, F.; Jahnke, A. A.; Stingelin, N.; Seferos, D. S.; Kim, J.-S. Effects of Side-Chain Length and Shape on Polytellurophene Molecular Order and Blend Morphology. *J. Phys. Chem. C* **2017**, *121*, 2088-2098.

(13) Moseguí González, D.; Raftopoulos, K. N.; He, G.; Papadakis, C. M.; Brown, A.; Rivard, E.; Müller-Buschbaum, P. Bandgap-Tuning in Triple-Chalcogenophene Polymer Films by Thermal Annealing. *Macromol. Rapid Commun.* **2017**, 38, 1700065/1-6.

(14) Fei, Z.; Han, Y.; Gann, E.; Hodsden, T.; Chesman, A. S. R.; McNeill, C. R.; Anthopoulos, T. D.; Heeney, M. Alkylated Selenophene-Based Ladder-Type Monomers via a Facile Route for High-Performance Thin-Film Transistor Applications. *J. Am. Chem. Soc.* **2017**, *139*, 8552-8561.

(15) Zander, M.; Kirsch, G. On the Phosphorescence of Benzologues of Furan, Thiophene, Selenophene, and Tellurophene: A Systematic Study of the Intra-Annular Internal Heavy-Atom Effect. *Z. Naturforsch. A* **1989**, *44*, 205-209.

(16) Ohshita, J.; Matsui, S.; Yamamoto, R.; Mizumo, T.; Ooyama, Y.; Harima, Y.; Murafuji, T.; Tao, K.; Kuramochi, Y.; Kaikoh, T.; Higashimura, H. Synthesis of Dithienobismoles as Novel Phosphorescence Materials. *Organometallics* **2010**, *29*, 3239-3241.

(17) Matsumoto, T.; Tanaka, K.; Tanaka, K.; Chujo, Y. Synthesis and Characterization of Heterofluorenes Containing Four-Coordinated Group 13 Elements: Theoretical and Experimental Analyses and Comparison of Structures, Optical Properties and Electronic States. *Dalton Trans.* **2015**, *44*, 8697–8707.

(18) Jia, W.-L.; Liu, Q.-D.; Wang, R.; Wang, S. Novel Phosphorescent Cyclometalated Organotin (IV) and Organolead (IV) Complexes of 2,6-Bis(2′-indolyl)pyridine and 2,6-Bis[2′-(7-azaindolyl)]pyridine. *Organometallics* **2003**, *22*, 4070–4078.

(19) Behrh, G. K.; Isobe, M.; Massuyeau, F.; Serier-Brault, H.; Gordon, E. E.; Koo, H. J.; Whangbo, M. H.; Gautier, R.; Jobic, S. Oxygen-Vacancy-Induced Midgap States Responsible for the Fluorescence and the Long-Lasting Phosphorescence of the Inverse Spinel $Mg(Mg,Sn)O_4$. *Chem. Mater.* **2017**, *29*, 1069–1075.

(20) Baldo, M. A.; Lamansky, S.; Burrows, P. E.; Thompson, M. E.; Forrest, S. R. Very High-Efficiency Green Organic Light-Emitting Devices Based on Electrophosphorescence. *Appl. Phys. Lett.* **1999**, *75*, 4-6.

(21) Chi, Y.; Chou, P.-T. Transition-Metal Phosphors with Cyclometalating Ligands: Fundamentals and Applications. *Chem. Soc. Rev.* **2010**, *39*, 638-655.

(22) Zhao, W.; He, Z.; Lam, J. W. Y.; Peng, Q.; Ma, H.; Shuai, Z.; Bai, G.; Hao, J.; Tang, B. Z. Rational Molecular Design for Achieving Persistent and Efficient Pure Organic Room-Temperature Phosphorescence. *Chem.* **2016**, *1*, 592-602.

(23) Ly, K. T.; Chen-Cheng, R.-W.; Lin, H.-W.; Shiau, Y.-J.; Liu, S.-H.; Chou, P.-T.; Tsao, C.-S.; Huang, Y.-C.; Chi, Y. Near-Infrared Organic Light-Emitting Diodes with Very High External Quantum Efficiency and Radiance. *Nat. Photonics* **2017**, *11*, 63-68.

(24) He, G.; Torres Delgado, W.; Schatz, D. J.; Merten, C.; Mohammadpour, A.; Mayr, L.; Ferguson, M. J.; McDonald, R.; Brown, A.; Shankar, K.; Rivard, E. Coaxing Solid-State Phosphorescence from Tellurophenes. *Angew. Chem., Int. Ed.* **2014**, *53*, 4587-4591.

(25) He, G.; Wiltshire, B. D.; Choi, P.; Savin, A.; Sun, S.; Mohammadpour, A.; Ferguson, M. J.; McDonald, R.; Farsinezhad, S.; Brown, A.; Shankar, K.; Rivard, E. Phosphorescence within Benzotellurophenes and Color Tunable Tellurophenes under Ambient Conditions. *Chem. Commun.* **2015**, *51*, 5444-5447.

(26) Braun, C. A.; Zomerman, D.; de Aguiar, I.; Qi, Y.; Torres Delgado, W.; Ferguson, M. J.; McDonald, R.; de Souza, G. L. C.; He, G.; Brown, A.; Rivard, E. Probing the Nature of Peripheral Boryl Groups within Luminescent Tellurophenes. *Faraday Discuss.* **2017**, *196*, 255-268.

(27) Mohammadpour, A.; Wiltshire, B. D.; Farsinezhad, S.; Zhang, Y.; Askar, A. M.; Kisslinger, R.; Delgado, W. T.; He, G.; Kar, P.; Rivard, E.; Shankar, K. Charge Transport, Doping and Luminescence in Solution-Processed, Phosphorescent, Air-Stable Tellurophene Thin Films. *Org. Electronics* **2016**, *39*, 153-162.

(28) Torres Delgado, W.; Shahin, F.; Ferguson, M. J.; McDonald, R.; He, G.; Rivard, E. Selective Placement of Bromide and Pinacolboronate Groups about a Tellurophene: New Building Blocks for Optoelectronic Applications. *Organometallics* **2016**, *35*, 2140-2148.

(29) Lapkowski, M.; Motyka, R.; Suwinski, J.; Data, P. Photoluminescent Polytellurophene Derivatives of Conjugated Polymers as a New Perspective for Molecular Electronics. *Macromol. Chem. Phys.* **2012**, *213*, 29-35.

(30) Koide, Y.; Kawaguchi, M.; Urano, Y.; Hanaoka, K.; Komatsu, T.; Abo, M.; Terai, T.; Nagano, T. A Reversible Near-Infrared Fluorescence Probe for Reactive Oxygen Species Based on Te–Rhodamine. *Chem. Commmun.* **2012**, *48*, 3091-3093.

(31) Kryman, M. W.; Schamerhorn, G. A.; Yung, K.; Sathyamoorthy, B.; Sukumaran, D. K.; Ohulchanskyy, T. Y.; Benedict, J. B.; Detty, M. R. Organotellurium Fluorescence Probes for Redox Reactions: 9-Aryl-3,6-diaminotelluroxanthylium Dyes and Their Telluroxides. *Organometallics* **2013**, *32*, 4321-4333.

(32) McCormick, T. M.; Carrera, E. I.; Schon, T. B.; Seferos, D. S. Reversible Oxidation of a Water-Soluble Tellurophene. *Chem. Commun.* **2013**, *49*, 11182-11184.

(33) Annaka, T.; Nakata, N.; Ishii, A. Synthesis, Structures, and Temperature-Dependent Photoluminescence of 1,4-Diphenyl-1-Telluro-1,3-butadiene Incorporated in a Dibenzobarrelene Skeleton and Derivatives. *Organometallics* **2015**, *34*, 1272-1278.

(34) Kremer, A.; Fermi, A.; Biot, N.; Wouters, J.; Bonifazi, D. Supramolecular Wiring of Benzo-1,3-chalcogenazoles through Programmed Chalcogen Bonding Interactions. *Chem. Eur. J.* **2016**, *22*, 5665-5675.

(35) Manjare, S. T.; Kim, Y.; Churchill, D. G. Selenium- and Tellurium-Containing Fluorescent Molecular Probes for the Detection of Biologically Important Analytes. *Acc. Chem. Res.* **2014**, *47*, 2985-2998.

(36) Yamaguchi, Y.; Nakata, N.; Ishii, A. Strong Solid-State Phosphorescence of 1,2-Telluraplatinacycles Incorporated into Rigid Dibenzobarrelene and Triptycene Skeletons. *Eur. J. Inorg. Chem.* **2013**, 5233–5239.

(37) Kryman, M. W.; McCormick, T. M.; Detty, M. R. Longer-Wavelength-Absorbing, Extended Chalcogenorhodamine Dyes. *Organometallics* **2016**, *35*, 1944–1955.

(38) Shoji, Y.; Ikabata, Y.; Wang, Q.; Nemoto, D.; Sakamoto, A.; Tanaka, N.; Seino, J.; Nakai, H.; Fukushima, T. Unveiling a New Aspect of Simple Arylboronic Esters: Long-Lived Room-Temperature Phosphorescence from Heavy-Atom-Free Molecules. *J. Am. Chem. Soc.* **2017**, *139*, 2728-2733.

(39) For an example of phosphorescence in BPin-appended organic compounds, see: Satou, M.; Nakamura, T.; Aramaki, Y.; Okazaki, S.; Murata, M.; Wakamiya, A.; Murata, Y. Near-Infrared Emissive Donor–Acceptor-Type Molecules Containing Thiazole-Fused Benzothiadiazole as an Electron-Acceptor Moiety. *Chem. Lett.* **2016**, *45*, 892-894.

(40) Ding, L.; Dong, S.-C.; Jiang, Z.-Q.; Chen, H.; Liao, L.-S. Orthogonal Molecular Structure for Better Host Material in Blue Phosphorescence and Larger OLED White Lighting Panel. *Adv. Funct. Mater.* **2015**, *25*, 645-650.

(41) Uchida, M.; Izumizawa, T.; Nakano, T.; Yamaguchi, S.; Tamao, K.; Furukawa, K. Structural Optimization of 2,5-Diarylsiloles as Excellent Electron-Transporting Materials for Organic Electroluminescent Devices. *Chem. Mater.* **2001**, *13*, 2680-2683.

(42) Zhang, F.; Zhao, X.; Yi, C.; Bi, D.; Bi, X.; Wei, P.; Liu, X.; Wang, S.; Li, X.; Zakeeruddin, S. M.; Grätzel, M. Dopant-Free Star-Shaped Hole-Transport Materials for Efficient and Stable Perovskite Solar Cells. *Dyes and Pigments* **2017**, *136*, 273-277.

(43) Liu, Y.; Chen, Q.; Duan, H.-S.; Zhou, H.; Yang, Y.; Chen, H.; Luo, S.; Song, T.-B.; Dou, L.; Hong, Z.; Yang, Y. A Dopant-Free Organic Hole Transport Material for Efficient Planar Heterojunction Perovskite Solar Cells. *J. Mater. Chem. A* **2015**, *3*, 11940-11947.

(44) Nishimura, H.; Ishida, N.; Shimazaki, A.; Wakamiya, A.; Saeki, A.; Scott, L. T.; Murata, Y. Hole-Transporting Materials with a Two-Dimensionally Expanded π-System around an Azulene Core for Efficient Perovskite Solar Cells. *J. Am. Chem. Soc.* **2015**, *137*, 15656–15659.

(45) Negishi, E.; Cederbaum, F. E.; Takahashi, T. Zirconocene Dichloride with Alkyllithiums or Alkyl Grignard Reagents as a Convenient Method for Generating a Zirconocene Equivalent and its Use in Zirconium-Promoted Cyclization of Alkenes, Alkynes, Dienes, Enynes, and Diynes. *Tetrahedron Lett.* **1986**, *27*, 2829-2832.

(46) Fagan, P. J.; Nugent, W. A. Synthesis of Main Group Heterocycles by Metallacycle Transfer from Zirconium. *J. Am. Chem. Soc.* **1988**, *110*, 2310-2312.

(47) Rosenthal, U.; Ohff, A.; Baumann, W.; Tillack, A.; Görls, H.; Burlakov, V. V.; Shur, V. B.; Struktur, Eigenschaften Und NMR-Spektroskopische Charakterisierung von $Cp_2Zr(Pyridin)(Me_3SiC{\equiv}CSiMe_3)$. *Z. Anorg. Allg. Chem.* **1995**, *621*, 77-83.

(48) Yan, X.; Xi, C. Conversion of Zirconacyclopentadienes into Metalloles: Fagan–Nugent Reaction and Beyond. *Acc. Chem. Res.* **2015**, *48*, 935-946.

(49) Dutton, J. L.; Farrar, G. J.; Sgro, M. J.; Battista, T. L.; Ragogna, P. J. Lewis Base Sequestered Chalcogen Dihalides: Synthetic Sources of ChX_2 (Ch = Se, Te; X = Cl, Br). *Chem. Eur. J.* **2009**, *15*, 10263–10271.

(50) For full crystallographic, computational and spectroscopic details, see the Supporting Information.

(51) Mei, J.; Leung, N. L. C.; Kwok, R. T. K.; Lam, J. W. Y.; Tang, B. Z. Aggregation-Induced Emission: Together We Shine, United We Soar! *Chem. Rev.* **2015**, *115*, 11718-11940.

(52) Lumpi, D.; Horkel, E.; Plasser, F.; Lischka, H.; Fröhlich, J. Synthesis, Spectroscopy, and Computational Analysis of Photoluminescent Bis(aminophenyl)-Substituted Thiophene Derivatives. *ChemPhysChem* **2013**, *14*, 1016–1024.

(53) Mantina, M.; Chamberlin, A. C.; Valero, R.; Cramer, C. J.; Truhlar, D. G. Consistent van der Waals Radii for the Whole Main Group. *J. Phys. Chem. A* **2009**, *113*, 5806-5812.

(54) Shynkaruk, O.; Qi, Y.; Cottrell-Callbeck, A.; Torres Delgado, W.; McDonald, R.; Ferguson, M. J.; He, G.; Rivard, E. Modular Synthesis of Diarylalkynes and Their Efficient Conversion into Luminescent Tetraarylbutadienes. *Organometallics* **2016**, *35*, 2232–2241.

(55) Shynkaruk, O.; He, G.; McDonald, R.; Ferguson, M. J.; Rivard, E. Modular Synthesis of Spirocyclic Germafluorene-Germoles: A New Family of Tunable Luminogens. *Chem. Eur. J.* **2016**, *22*, 248–257.

(56) Muhkerjee, S.; Thilagar, P. Recent Advances in Purely Organic Phosphorescent Materials. *Chem. Commun.* **2015**, *51*, 10988-11003.

(57) Ravotto, L.; Ceroni, P. Aggregation Induced Phosphorescence of Metal Complexes: From Principles to Applications. *Coord. Chem. Rev.* **2017**, *346*, 62-76.

(58) Samanta, S.; Basu Roy, M.; Chatterjee, M.; Ghosh, S. Simultaneous Emissions from T_2 and T_1 States of Naphthalene Moiety in a Specially Designed Naphthalene Cryptand. *J. Lumines.* **2007**, *126*, 230-238; at this point we cannot rule out that some luminescence in **Fl-Te-6-Fl** is still mediated via excimer formation as attempts to record luminescence data from **Fl-Te-6-Fl** in PMMA films and in the presence of benzophenone as a triplet sensitizer gave weak/poorly resolved data.

(59) While we designate singlet and triplet states with the labels S and T, due to the substantial spin-orbit coupling instigated by the heavy Te atoms, pronounced mixing between these excited states occurs. For a detailed study on the role of spin-orbit coupling on the phosphorescence of tellurophenes, see reference 26.

(60) Kasha, M. Characterization of Electronic Transitions in Complex Molecules. *Discuss. Faraday Soc.* **1950**, *9*, 14-19.

(61) In addition to examining the initial excitation step, computational determination of the phosphorescence wavelengths (energies) has been carried out for a number of the phosphorescent compounds (Table S17).[50] The phosphorescence energies have been taken as the energy difference between the optimized lowest energy triplet state (as determined with UB3LYP/CC-PVTZ-(PP)) and the singlet ground state, including zero-point energy corrections. The computed phosphorescence energies were typically within 0.04-0.15 eV of the experimental measurements; a notable exception was **TPA-6-Te-TPA**, where intermolecular interactions are thought to play an important role.

(62) Pangborn, A. B.; Giardello, M. A.; Grubbs, R. H.; Rosen, R. K.; Timmers, F. J. Safe and Convenient Procedure for Solvent Purification. *Organometallics* **1996**, *15*, 1518-1520.

(63) Jantunen, K. C.; Scott, B. L.; Kiplinger, J. L. A Comparative Study of the Reactivity of Zr(IV), Hf(IV) and Th(IV) Metallocene Complexes: Thorium Is Not a Group IV Metal after All. *J. Alloy Compd.* **2007**, *444-445*, 363-368.

(64) Gudeika, D.; Grazulevicius, J. V.; Volyniuk, D.; Juska, G.; Sini, G. Effect of Ethynyl Linkages on the Properties of the Derivatives of Triphenylamine and 1,8-Naphthalimide. *J. Phys. Chem. C* **2015**, *119*, 28335-28346.

(65) Linshoeft, J.; Baum, E. J.; Hussain, A.; Gates, P. J.; Näther, C.; Staubitz, A. Highly Tin-Selective Stille Coupling: Synthesis of a Polymer Containing a Stannole in the Main Chain. *Angew. Chem., Int. Ed.* **2014**, *53*, 12916–12920.

(66) Van Overmeire, I.; Boldin, S. A.; Venkataraman, K.; Zisling, R.; De Jonghe, S.; Van Calenbergh, S.; De Keukeleire, D.; Futerman, A. H.; Herdewijn, P. Synthesis and Biological Evaluation of Ceramide Analogues with Substituted Aromatic Rings or an Allylic Fluoride in the Sphingoid Moiety. *J. Med. Chem.* **2000**, *43*, 4189–4199.

(67) Xiao, H.; Shen, H.; Lin, Y.; Su, J.; Tian, H. Spirosilabifluorene Linked Bistriphenylamine: Synthesis and Application in Hole Transporting and Two-Photon Fluorescent Imaging. *Dyes and Pigments* **2007**, *73*, 224–229.

(68) Allen, M. W. Measurement of Fluorescence Quantum Yields, Thermo Fisher Scientific technical note 52019, Madison, WI, USA.

(69) Rhys Williams, A. T.; Winfield, S. A.; Miller, J. N. Fluorescence Quantum Yields Using a Computer-Controlled Luminescence Spectrometer. *Analyst* **1983**, *108*, 1067–1071.

(70) Park, K.; Bae, G.; Moon, J.; Choe, J.; Song, K. H.; Lee, S. Synthesis of Symmetrical and Unsymmetrical Diarylalkynes from Propiolic Acid Using Palladium-Catalyzed Decarboxylative Coupling. *J. Org. Chem.* **2010**, *75*, 6244–6251.

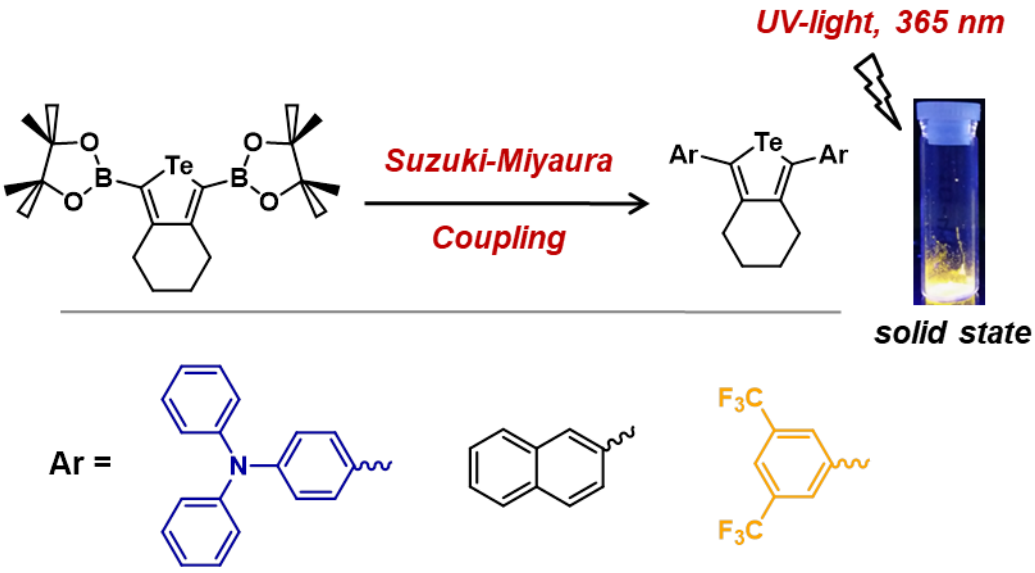
UV-light, 365 nm
Suzuki-Miyaura
Coupling
Ar
Te
Ar
solid state
Ar =
N
F3C
F3C